

Stabilization Operation Region and Operational Variables Effect on a Reciprocal Flow Burner

VALERI BUBNOVICH, LUIS HENRÍQUEZ, CATALINA DÍAZ, EMILIO ÁVILA

Department of Chemical Engineering

University of Santiago of Chili

B. O'Higgins 3363, Santiago

CHILI

valeri.bubnovich@usach.cl <http://www.usach.cl>

Abstract: - A reciprocal gas flow burner is computationally simulated for obtaining its stable operation region in terms of equivalence ratio and filtration velocity, for two energy losses configurations schemes. Equivalence ratio and filtration velocity were considered over the range [0.1, 1.0] and [0.25, 1.0] (m/s). The one-dimensional mathematical model consider that porous media is made by alumina bolls of 5.6 mm diameter, which fill up a quartz hollow cylinder of 5 cm diameter and 50 cm high. The mathematical model includes total mass preservation laws, momentum and enthalpy for the solid as for the gas. Combustion is modeled through global chemical reaction in one step. Chemical kinetic of methane combustion is treated on the base of Arrhenius approximation. It is considered besides that system heat transport occurs at conditions without local thermal equilibrium and includes convections mechanisms, conduction and thermal radiation. Lateral heat losses from the system to environment through cylinder lateral surface were studied at two scenarios: reactor coupled with and without heat exchangers. Mathematical model are discretized by finite differences method through implicit scheme and its solution reached by TDMA algorithm. Uniform grid with 801 nodes and time step $\Delta t = 0.01$ (s) gave solution independence. Results demonstrated increased stabilization in temperature profile, thus increased stabilization region for the reactor coupled with heat exchangers.

Key-Words: - Reciprocal Flow Burner (RFB); porous media; filtration combustion; numerical simulation

1 Introduction

Because of the pressure derived from the need to lower emissions and increase efficiency in the combustion of fossil fuels, new methods of combustion and advanced burner designs are being sought.

A porous medium burner can provide a good solution because it has a number of advantages compared to conventional combustion with a free flame: large power variation range, high efficiency, compact structure with very high energy concentration per unit volume, extremely low CO and NO_x emission over a wide range of thermal loads, stable combustion over a wide range of equivalence ratios, $0.4 < \Phi < 0.9$ [1-2]. All the arguments mentioned above are driving the current development of these kinds of burners which have already found several important industrial applications [3-5].

The problem of gas combustion in inert porous media has been studied intensively both theoretically and experimentally. The most important results of

both research methodologies have been summarized [6, 7].

One of the most important problems of porous media burners is stabilization of the flame in a specific zone of the inert porous medium. It is also important for the static combustion front to have some predefined characteristics to be able to maximize the efficiency of the burner and minimize CO and NO_x emissions [4].

For that purpose four different flame control methods have been developed. The first method considers the formation of two layers of the porous medium in which the modified Peclet number is less than (first layer) or greater than (second layer) 65 [1, 3, 8]. The second method considers cooling of the postcombustion zone [9, 10]. The third method allows retaining the flame in a specific zone of the porous medium by means of a periodic exchange of the mixture inlet and the exhaust of the combustion gases [11-13]. Finally, the fourth method of flame stabilization employs a porous body with non-constant cross sectional area [14].

The motion of the combustion zone results in positive or negative enthalpy fluxes between the

reacting gas and solid porous media. As a result, observed combustion temperatures can significantly differ from adiabatic predictions based on the enthalpy of the initial reactants and is controlled mainly by reaction chemistry and heat transfer mechanism. Upstream wave propagation, countercurrent to the gas flow, results in superadiabatic combustion temperature [6] while downstream propagation of the wave leads to combustion in the superadiabatic regime with temperatures much in excess of the adiabatic temperature [12]. Superadiabatic combustion significantly extends conventional flammability limits to the region of ultra low heat content mixtures.

Reciprocating superadiabatic combustion of premixed gases in porous media is a new porous burner technology. With embedded devices periodically switching the direction of the premixed gases, a reciprocal flow burner (RFB) not only has the advantages of a porous media burner with one-directional flow, but also some more attractive combustion characteristics [15]. The main principal advantages of RFB are attributed to dual heat recuperation effects. Burners in which heat is recirculated produce large excess enthalpies in hopes of achieving higher local combustion temperatures and higher thermodynamic efficiencies without attaining high temperatures at the exit of the burner. Through this dual heat recirculation it is theoretically possible to achieve a local temperature beyond the adiabatic flame temperature of the mixture entering the burner. Porosities and structures of the porous media (PM) may have dominating effects on the RFB performance.

Consequently, a RFB burner with good performance regarding a high temperature zone and moderate pressure loss may be achieved through sophisticated designing and improving the structure of the burners. In order to improve and optimize the combustion processes in the PM burners, experimental and numerical investigations have been intensively conducted in recent years.

Homogeneous porous media consisting either of ceramic foams or of alumina pellets are generally used in experimental studies [11, 16]. Hanamura and Echigo [17] carried out the first numerical study on the combustion characteristics of the RFB system. Brenner et al. [9] investigated a 10-KW PM burner with an integrated heat exchanger unit. Malico et al. [18] used a two-dimensional model to simulate an integrated burner with a heat exchanger. Contarin et al. [12, 19] studied a Reciprocal Flow Burner (RFB) with embedded heat exchangers; they applied a one-dimensional two-phase model with one-step kinetics

to test a new concept of heat extraction strategy. It was shown that the heat extraction efficiency increased from 70% to 80%, as the equivalence ratio increased in the range $0.1 < u < 1.0$ and that the pollutant emissions were very low. Howell et al. [7] analyzed the modeling assumptions employed in the PM combustion and pointed out that the no-radial-heat-loss assumption was probably the most inaccurate among those assumptions. Therefore, a detailed modeling heat loss from the system is imperative. Jugjai et al. [20, 21] examined both experimentally and numerically the combustion and heat transfer characteristics in a RFB burner, comparisons were made to those of a PM burner with uni-directional flow.

In [15], an experimental work was performed at first to deepen the understanding of the RFB characteristics. Subsequently, numerical simulations were performed in order to clarify the complex heat transfer mechanisms and to gain some guidance for the design of the PM combustor. Attention was focused on the combustion temperature and pressure loss in the burner, which was, respectively, packed with 4PPC (Pores Per Centimeter) ceramic foams or alumina pellets with various sizes. Results show that material and structures of porous media have significant influence on the burner performance, and that ceramic foam with high porosity is suitable for using in the combustion region whereas alumina pellets should be placed in the heat exchange zone. In addition, the highly two-dimensional characteristics of the porous media burner are validated by the numerical model, which include temperature distributions, species profile and flame structure.

Based on the analogy with the steady countercurrent reactor, a simplified theoretical solution is presented in [22], which is applicable to adiabatic inert porous media combustors with reciprocating flow. Results show that the lean flammability limit can be extended by using porous media of smaller pore size. The predicted lean flammability limit provides guidelines for the design of the combustor and some indications for further improving the combustor performances. The influences of thermo physical properties of porous media on superadiabatic combustion with reciprocating flow is numerically studied in order to improve the understanding of the complex heat transfer and optimum design of the combustor. Several series of simulations are run with the purpose of investigating the influence of the most important thermo physical parameters: specific heat, thermal conductivity, extinction coefficient,

volumetric convective heat transfer coefficient, and wall heat loss coefficient.

A new system for converting combustion heat into electric power is proposed in [24] on the basis of reciprocating flow superadiabatic combustion in a catalytic and thermoelectric porous element. In the combustion system, a trapezoidal temperature distribution is established along the low direction, resulting in a steep temperature gradient in the thermoelectric porous element. The total thermal efficiency reaches 4.7%.

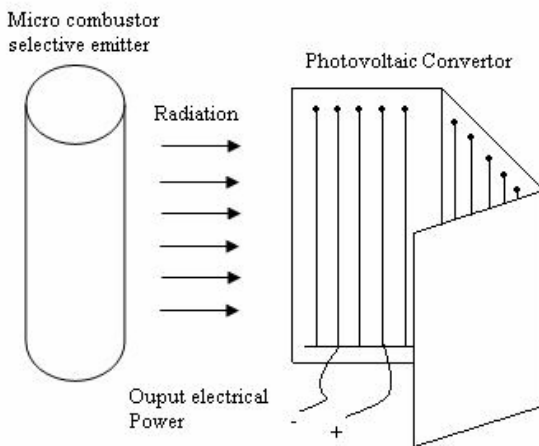


Figure 1: Schematic representation of a TPV system.

Fast depleting reserves of conventional energy sources has resulted in an urgent need for increasing energy conversion efficiencies and recycling of waste heat. One of the potential candidates for fulfilling these requirements is thermo photovoltaic (TPV) devices. TPV devices generate electricity from either the complete combustion of different fuels or the waste heat of other energy sources, thereby saving energy. TPV technology is based in direct conversion from thermal radiation to electric energy through photovoltaic (PV) cells. These systems are composed of a thermal radiation source, a selective photon emitter, a band photon filter and a photovoltaic converter [25]. The selective emitter and filter adapt the radiation spectrum to a maximum photon absorption in PV cells. Absence of any moving parts and versatile fuel usage has made TPV devices very appealing for different applications. However, the presently available TPV systems suffer from low conversion efficiency.

The present work has as objective the study of a RFB with porous media body conformed of alumina spheres with 5.6 mm diameter that can be used as energy source for a TPV system.

1 Problem Formulation

The reciprocal flow burner consists of a quartz tube of length $L = 50$ (cm), outer diameter $d_t = 50$ (mm), filled with randomly disposed alumina spheres of diameter $d_0 = 5.6$ (mm), giving volumetric porosity $m = 0.4$.

In this type of reactor confinement of the combustion wave is achieved by periodically reversing the mixture fuel / oxidizer flow direction. The parameter t_c , represents the half cycle time of the system, namely, each time instant t_c reverses the gas mixture flow direction.

Its main feature is the ability to combust mixtures with a very low calorific value given the right conditions for energy losses to the external environment.

Two cases of lateral energy losses were studied for parameter β ($\text{W}/\text{m}^3\text{K}$). First configuration considered two heat exchangers of length $L_L = L_R = 12$ (cm) placed at the left and right reactor ends. Central part was kept under isolation in order to maintain constant temperature profiles in this region. Second reactor configuration was not coupled with heat exchangers and thus, according to an energy balance to the reactor, volumetric heat losses are function of the temperature $\beta = f(T)$ as shown in Eq. (1).

$$\beta = \frac{4}{d_{tubo} (T_s - T_{ext})} \left(\varepsilon \cdot \kappa \cdot \sigma (T_s^4 - T_{ext}^4) + \alpha_{out} (T_s - T_{ext}) \right) \quad (1)$$

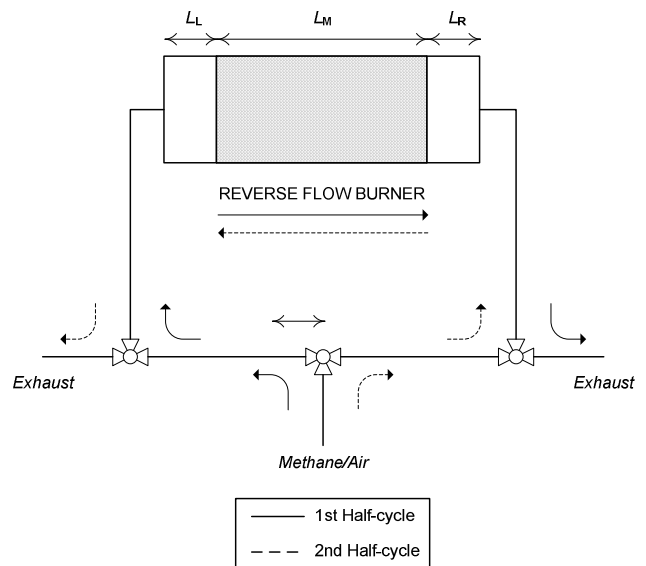
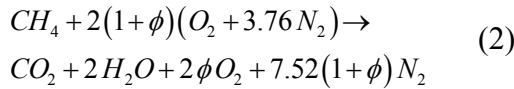


Figure 2: Reciprocal flow burner.

Fig. 2 shows reactor left, middle and right regions considered; where T_s , T_{ext} are porous media and extern temperature, ε alumina emissivity, κ quartz tube transmissivity, α_{out} heat transfer coefficient from cylindrical mantle.

2.1 Governing equations

Inside reactor RFB, temperature and composition profiles are assumed one-dimensional. Chemical reaction of combustion (CH_4/Air) is homogenous and one-step kinetics model of Eq. (2) applies:



Where $\Phi = (1+\phi)^{-1}$ is the equivalence ratio.

2.1.1 Continuity Equation

$$\frac{\partial(\rho_g \cdot u_g)}{\partial z} = 0 \quad (3)$$

Where u_g is the filtration velocity of gas mixture. Here is assumed ideal gas behavior due to operating conditions of low pressures ($\sim 1\text{atm}$) and high temperatures (1300 – 1800 K):

$$\rho_g = \frac{p \cdot M}{R \cdot T_g} \quad (4)$$

With p atmospheric pressure (atm), M average molar mass of gas mixture (g/mol), R universal gas constant (atm·L/mol·K), T_g gas phase temperature (K).

2.1.2 Mass conservation of fuel

$$\rho_g \frac{\partial w_i}{\partial t} + \rho_g \cdot u_g \frac{\partial w_i}{\partial z} = \frac{\partial}{\partial z} \rho_g \cdot D \frac{\partial w_i}{\partial z} + r_i \quad (5)$$

$$D = D_g + D_d \quad (6)$$

$$D_d = 0.5 \cdot u_g \cdot d_o \quad (7)$$

With w_i mass fraction of methane, D_g gas diffusivity, D_d axial dispersion coefficient. Consumption rate of

fuel is given by Eq. (8):

$$r_i = -K_0 \cdot w_i \cdot \rho_g \exp(-E/R \cdot T_g) \quad (8)$$

Frequency factor and activation energy are $K_0 = 2.6 \cdot 10^8$ (1/s), $E/R = 15643.5$ (K).

2.1.3 Gas phase energy conservation

Heat transfer mechanisms by convection, conduction and dispersion are considered, and additional term of heat release due to reaction of combustion is included in formulation:

$$\begin{aligned} \rho_g \cdot c_p \frac{\partial T_g}{\partial t} + c_p \cdot \rho_g \cdot u_g \frac{\partial T_g}{\partial z} - \\ \frac{\partial}{\partial z} (\lambda_g + D_d \cdot \rho_g \cdot c_p) \frac{\partial T_g}{\partial z} = \frac{\alpha_{vol}}{m} (T_s - T_g) - r_i \cdot \Delta h_c \end{aligned} \quad (9)$$

Boundary and initial conditions are given by:

$$\forall t, \quad \frac{\partial T_g}{\partial z} \Big|_{z=0,L} = 0 \quad (10)$$

$$t = 0, \quad T_g \Big|_{z=z} = T_0 \quad (11)$$

Where c_p , λ_g heat capacity and conductivity of gas mixture, α_{vol} volumetric heat transfer coefficient between solid and gas phases, Δh_c heat of reaction, T_0 , T_s initial and solid temperature respectively. Physical properties of gas mixture are correlated by Eqs. (12)-(15):

$$c_p = 947.0 \cdot \exp(1.83 \cdot 10^{-4} \cdot T_g) \quad (12)$$

$$\lambda_g = 4.82 \cdot 10^{-7} \cdot c_p \cdot T_g^{0.7} \quad (13)$$

$$\alpha_{vol} = \frac{\lambda_g \cdot 6(1-m)}{d_o^2} \left[2 + 1.1 \left(\frac{\mu \cdot c_p}{\lambda_g} \right)^{1/3} \left(\frac{\rho_g \cdot m \cdot u_g \cdot d_o}{\mu} \right)^{0.6} \right] \quad (14)$$

$$\mu = 3.37 \cdot 10^{-7} \cdot T_g^{0.7} \quad (15)$$

With μ gas mixture viscosity.

2.1.4 Solid phase energy conservation

Heat transfer by conduction, radiation and interphase heat exchange are included:

$$(1-m)\rho_s \cdot c_s \frac{\partial T_s}{\partial t} - \frac{\partial}{\partial z} \left(\lambda \frac{\partial T_s}{\partial z} \right) = \alpha_{vol}(T_g - T_s) - \beta(T_s - T_{ext}) \quad (16)$$

$$\lambda = 0.01 \cdot \lambda_s + \frac{32 \cdot \sigma \cdot d_0 \cdot m \cdot \varepsilon}{9(1-m)} T_s^3 \quad (17)$$

Initial and boundary conditions given by:

$$T_s|_{t=0} = \begin{cases} T_{ign}, z \in [z_-; z_+] \\ T_0, z \notin [z_-; z_+] \end{cases} \quad (18)$$

$$\left. \frac{\partial T_s}{\partial z} \right|_{z=0,L} = 0 \quad (19)$$

Here T_{ign} ignition temperature, σ Stefan-Boltzmann constant, c_s , λ_s heat capacity and thermal conductivity of solid phase correlated by:

$$c_s = 29.567 + 2.61177 \cdot T_s - 0.00171 \cdot T_s^2 + 3.382 \cdot 10^{-7} \cdot T_s^3 \quad (20)$$

$$\lambda_s = -0.21844539 + 0.00174653 \cdot T_s + 8.2266 \cdot 10^{-8} \cdot T_s^2 \quad (21)$$

2.2 Numerical solution of equations

Mathematical model are discretized by finite differences method through implicit scheme and its solution reached by TDMA algorithm. Uniform grid with 801 nodes and time step $\Delta t = 0.01$ (s) gave solution independence.

2.3 Numerical validation

Validation of numerical solution was reached through replication of results published in [12]. Fig. 3 presents gas and solid temperature profiles for $\phi = 2.33$, $u_g = 0.5$ (m/s), $t_c = 10$ (s). Temperature distributions found are in concordance to the results of Contarin et al [10], Fig. 4.

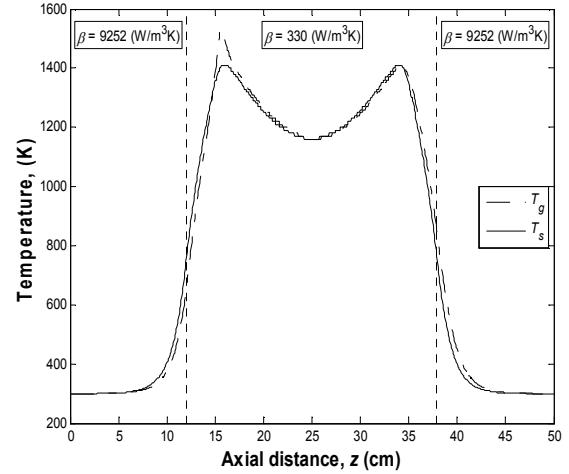


Figure 3: Gas and solid temperature profiles for validation, $\phi = 2.33$, $u_g = 0.5$ (m/s), $t_c = 10$ (s).

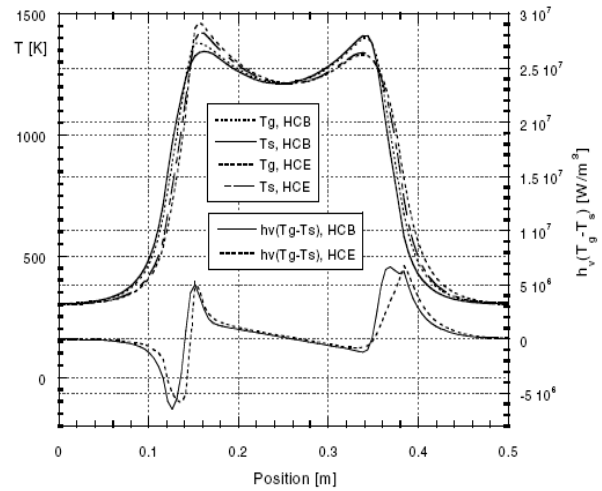


Figure 4: Temperature evolution during half cycle of the RFB: $u_g: m = 0.2$ (m/s), $\Phi = 0.3$. The acronyms HCB and HCE stand for the half cycle beginning and the half cycle end [12].

3 Problem Solution

3.1 Stable and unstable cases

Fig. 5 shows stable solid temperature evolution. Stationary temperature profiles were reached within the first 2000 (s). Situations depicted in Fig. 6 and Fig. 7 exhibits instabilities in the temperature profile which leads to unstable reactor operation. These scenarios are to be avoided, thus it is necessary to obtain the stability region for safe reactor operation.

3.2 Numerical simulation method

Simulations were performed in the space $u_g \in [0.25, 1]$ (m/s), $\Phi \in [0.1, 1]$, varying operational variables at steps of size $\Delta u_g = 0.02$ (m/s), $\Delta \Phi = 0.02$. Initially, for each case, an ignition profile is imposed in the central region of the reactor. A case for which the triplet (u_g, Φ, β) produces stable temperature profiles were recognized if variation of maximum temperature levels and position are kept under tolerances: $\Delta T_{s,Max} \leq 2$ (K) $\Delta z_w \leq 10^{-5}$ (m).

Unstable cases were detected if $T_{s,Max} \leq 800$ (K), condition of Fig. 6, or $z_{w,L} < 0.12$ (m), $z_{w,R} > 0.38$ (m) case of Fig. 7. The stability criteria were evaluated each 500 (s) starting from simulation time 2000 (s). Simulation time was extended until a stopping criterion was found, point at which a new triplet (u_g, Φ, β) was sought for evaluation.

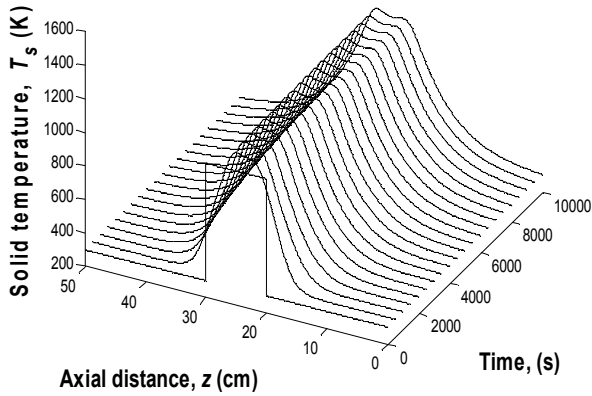


Figure 5: Stable temperature evolution inside reactor $u_g = 0.25$ (m/s), $\Phi = 0.25$, $\beta = f(T)$.

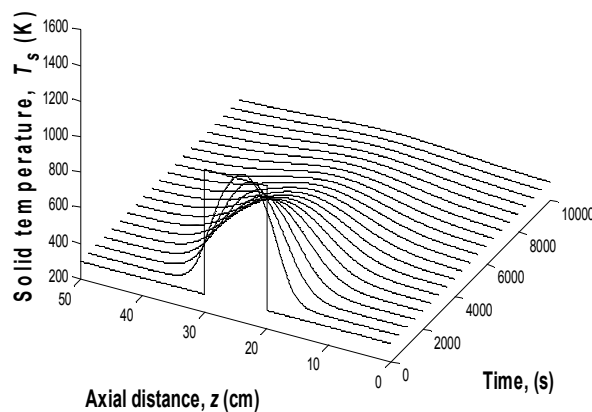


Figure 6: Unstable temperature evolution inside reactor $u_g = 0.25$ (m/s), $\Phi = 0.1$, $\beta = f(T)$.

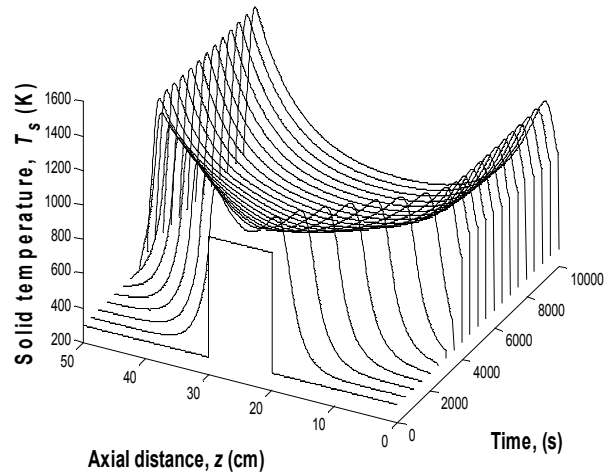


Figure 7: Unstable temperature evolution inside reactor $u_g = 0.5$ (m/s), $\Phi = 0.5$, $\beta = f(T)$.

3.3 Stability region

Fig. 8 presents stable operation region in the u_g - Φ plane for RFB reactor as function of type of energy losses. Firing rate contours are included for comparison of potency ranges between the two regions.

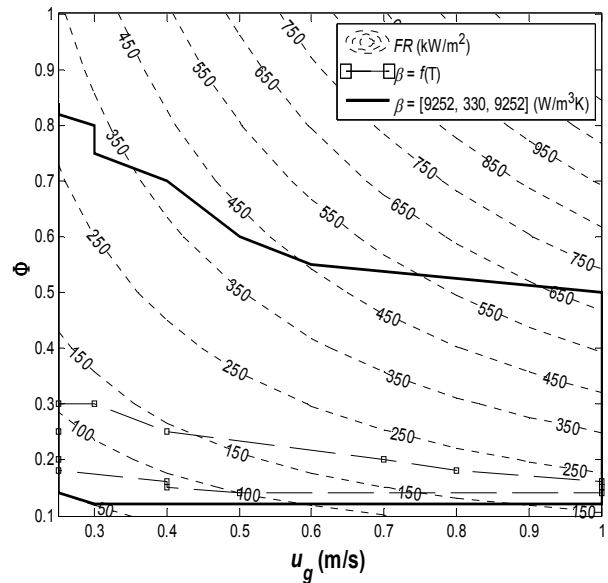


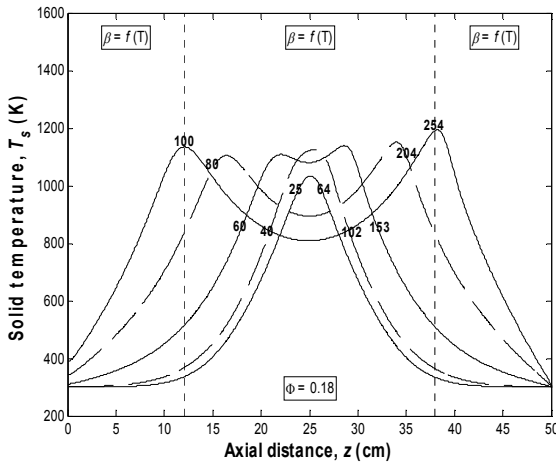
Figure 8: Stability operation regions for RFB reactor as function of energy losses. Numbers indicate values of firing rate in (kW/m²).

Results indicate a much larger stable operation region for the reactor coupled with heat exchangers. Firing rate range found for this type of energy losses was [50, 694] (kW/m²). Reactor with natural energy

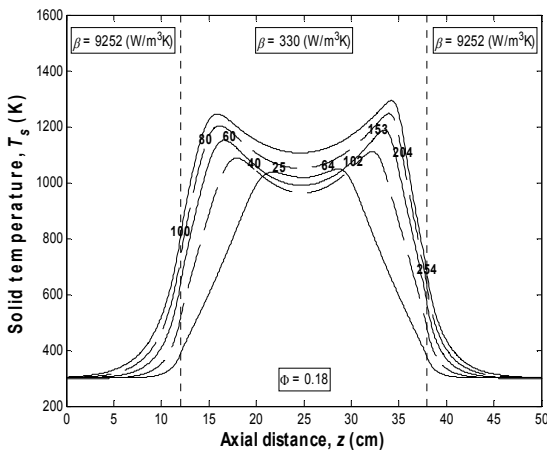
losses provides a much smaller potency range [64, 227] (kW/m²).

Similar lower region bound was found in both configurations, while the upper region bound found makes the most significant increment in operation range. These results indicate the stabilization effect that the coupled heat exchangers provide to the flame structure, which is most noticeable when the case to be stabilized is of the kind presented in FIG 7, i.e., an energy excess input to the central flame structure that causes to disrupt the plateau-shape temperature profile.

3.4 Operating variables variation effect on the thermal profiles



(a)



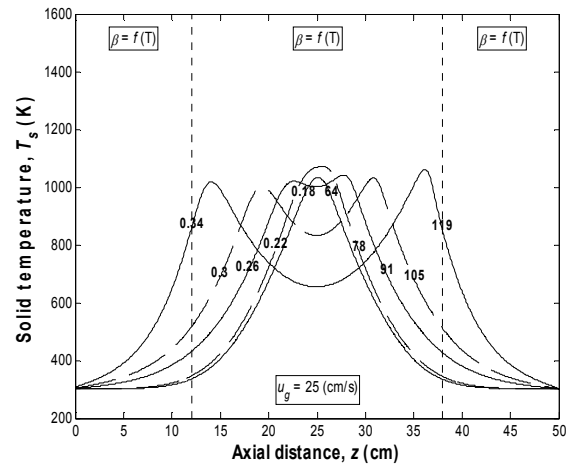
(b)

Figure 9: Effect of u_g in temperature profiles, (a) $\beta =$

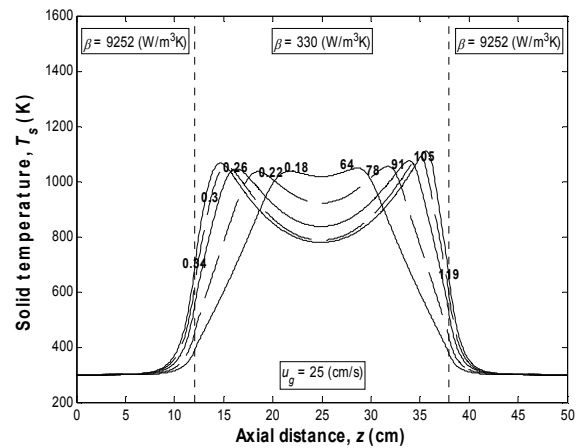
$f(T)$; (b) $\beta = [9252, 330, 9252]$. Numbers on the left and

right indicate values of u_g in (cm/s) and FR in (kW/m²),

respectively.



(a)



(b)

Figure 10: Effect of Φ in temperature profiles, (a) $\beta =$

$f(T)$; (b) $\beta = [9252, 330, 9252]$. Numbers on the left and

right indicate values of Φ and FR in (kW/m^2), respectively.

Fig. 9 presents the filtration velocity effect on the

thermal profiles within stabilization regions, $\beta = f(T)$

and $\beta = [9252, 330, 9252]$ ($\text{W/m}^3\text{K}$), for $\Phi = 0.18$.

Fig. 10 presents the equivalence ratio effect on the thermal profiles, within stabilization regions, for $u_g = 0.25$ (cm/s).

The general trend observed is the increase in thermal levels in the burner central region with the

increase of u_g and Φ . This result is expected because

the energy input increases with the operation variables. The shape of the thermal profiles is affected by the type of energy losses. The preheating region and the relation $T_{s,\text{m}\acute{\text{a}}\text{x}} / T_{s}|_{z=L/2}$ were greater for

the case $\beta = f(T)$.

Consequently the temperature profiles for the

situation described by $\beta = [9252, 330, 9252]$ possess

a form of plateau, namely, a higher central thermal level with a fast decay from its maximum to the external temperature at both ends. This form of thermal profile would be appropriate for applications where it is desired to maintain an approximately constant thermal level in the reactor central region, namely, conversion to electrical energy by thermo-

photovoltaic cells, catalytic reactions, amongst others.

4 Conclusions

A reciprocal flow burner for methane/air mixtures was computationally simulated for obtaining its stability operation region as function of energy losses to the external media. Results indicate a much larger operation range when heat exchangers are coupled at the reactors left and right regions compared to operation with natural heat losses. Similar lean flammability limits were found for both configurations whereas upper bound is noticeable higher for reactor coupled with heat exchangers.

With increasing operation variables u_g , Φ increase in thermal levels is achieved within the system. The developed thermal profile shape is a strong function

of the energy losses type. For the reactor coupled

with heat exchangers, thermal profiles show a more compact structure, similar to a plateau, which may be suited for the applications previously discussed due to its constant temperature central region.

5. Nomenclature

5.1 List of symbols

c	Specific heat
d_0	Particle diameter
d_{tube}	Reactor inner diameter
D_d	Dispersion coefficient
D_g	Molecular diffusivity coefficient
E	Activation energy
K_0	Frequency factor
L	Tube length
m	Porosity
M	Average gas molar mass
p	Atmospheric pressure
R	Universal gas constant
r_i	Consumption rate of methane
t	Time
u	Filtration velocity
w_i	Mass fraction of methane
z	Axial direction

5.2 Greek letters

α_{out}	Heat transfer coefficient at cylindrical mantle surface
α_{vol}	Volumetric heat transfer coefficient between

	phases
β	Volumetric energy losses coefficient to the environment
ρ	Density
ε	Emissivity of alumina spheres
ϕ	Fraction of excess air
Φ	Equivalence ratio
λ	Thermal conductivity
Δh_c	Specific reaction heat of methane
μ	Gas mixture viscosity
κ	Transmissivity of quartz tube
σ	Stefan-Boltzmann constant

5.3 Subscripts

w	Relative to temperature peak
L	Left
M	Middle
R	Right
Max	Maximum
s	Medium porous
g	Gaseous Mixture
0	Initial
ign	Ignition

Acknowledgements

The authors acknowledge the support of CONYICIT-Chile under FONDECYT project 1090550.

References:

- [1] S. Mößbauer, O. Pickenäcker, K. Pickenäcker, D. Trimis, Application of the Porous Burner Technology in Energy and Heat - Engineering. *Fifth International Conference on Technologies and Combustion for a Clean Environment (Clean Air V), Lisbon (Portugal)*, vol. 1, Lecture 20.2, 1999, pp. 519-523.
- [2] Valeri I. Bubnovich, Mario Toledo, Experimental Study of a Diluted Methane – Air Mixture Combustion under Filtration in a Packed Bed, *IASME Transactions*, Issue 3, Vol. 1, 2004, pp. 574 – 577.
- [3] D. Trimis, F. Durst, Combustion in a porous medium-advances and applications, *Combustion Science and Technology*, vol. 121, 1997, pp.153 – 168.
- [4] Mario Toledo, Valeri Bubnovich, Alexei Saveliev, Lawrence Kennedy, Filtration Combustion of Methane, Ethane, and Propane Mixtures with Air, *WSEAS Transactions on Heat and Mass Transfer*, Issue 3, Vol. 1, 2006, pp. 283 – 292.
- [5] K. V. Dobrego, N. N. Gnesdilov, I. M. Kozlov, V. I. Bubnovich, H. A. Gonzalez, Numerical investigation of the new regenerator – recuperator scheme of VOC oxidizer, *International Journal of Heat and Mass Transfer*, vol. 48, 2005, pp. 4695-4703.
- [6] V. S. Babkin, Filtrational combustion of gases. Present state of affairs and prospects, *Pure & Applied Chemistry*, vol. 65, No. 2, 1993, pp. 335-344.
- [7] J. R. Howell, M. J. Hall, J. L. Ellzey, Combustion of hydrocarbon fuel within porous inert media, *Progress in Energy Combustion Science*, vol. 22, 1996, pp.121-145.
- [8] V. S. Babkin, A. A. Korzhavin, V. A. Bunev, Propagation of Premixed Gaseous Explosion Flames in Porous Media, *Combustion and Flame*, vol. 87, 1991, pp.182-190.
- [9] G. Brenner, K. Pickenäcker, O. Pickenäcker, D. Trimis, K. Wawrzinek, T. Weber, Numerical and Experimental Investigation of Matrix-Stabilized Methane/Air Combustion in Porous Inert Media, *Combustion and Flame*, vol. 123, 2000, pp. 201-213.
- [10] P. H. Bouma, L. P. H. De Goey, Premixed Combustion on Ceramic Foam Burners, *Combustion and Flame*, 119, 1999, pp. 133-143.
- [11] J. G. Hoffmann, R. Echigo, H. Yoshida, S. Tada, Experimental Study on Combustion in Porous Media with a Reciprocating Flow System, *Combustion and Flame*, vol. 111, 1997, pp. 32-46.
- [12] F. Contarin, A. V. Saveliev, A. A. Fridman, L. A. Kennedy, A reciprocal flow filtration combustor with embedded heat exchangers: numerical study, *International Journal of Heat and Mass Transfer*, vol. 46, 2003, pp. 949-961.
- [13] Valeri Bubnovich, Luis Henriquez, Catalina Diaz, Emilio Avila, Stabilization Operation Region for a Reciprocal Flor Burner, *Recent Advances in Applied and Theoretical Mechanics, Proceedings of the 5th WSEAS International Conference on Applied and Theoretical Mechanics (Mechanics'09), Puerto De La Cruz, Tenerife, Canary Islands, Spain, December 14-16, 2009*, pp. 114-119.
- [14] S. A. Zhdanok, K. V. Dobrego, S. I. Foutko, Flame localization inside axis-symmetric cylindrical and spherical porous media burners, *International Journal of Heat and Mass Transfer*, vol. 41, 1998, pp. 3647-3655.

- [15] Mao-Zhao Xie, Jun-Rui Shi, Yang-Bo Deng, Hong Liu, Lei Zhou, You-Ning Xu, Experimental and numerical investigation on performance of porous medium burner with reciprocating flow, *Fuel*, Vol. 88, 2009, pp. 206-213.
- [16] S. Zhdanok, L.A. Kennedy, G. Koester, Superadiabatic combustion of methane air mixtures under filtration in a packed bed, *Combustion and Flame*, Vol. 100, 1995, pp. 221-31.
- [17] K. Hanamura, R. Echigo, Superadiabatic combustion in a porous medium, *International Journal of Heat and Mass Transfer*, Vol. 36, N 13, 1993, pp. 3201-3209.
- [18] I. Malico, X. Y. Zhou, J. C. F. Pereira, Two-dimensional numerical study of combustion and pollutants formation in porous burner, *Combustion Science Technology*, Vol. 152, 2000, pp. 57-79.
- [19] F. Contarin, W. M. Barcellos, A. V. Saveliev, L. A. Kennedy, Energy extraction from a porous media reciprocal flow burner with embedded heat exchangers, *Heat Mass Transfer*, Vol. 127, N 2, 2005, pp. 123-30.
- of a micropower (micro-thermophotovoltaic), *Journal of Power Sources*, vol. 165, 2007, pp. 455-480.
- [20] S. Jugjai, S. Wongveera, T. Teawchaitiporn, K. Limbwormsin, The surface combustor-heater with cyclic flow reversal combustion, *Experimental Thermal and Fluid Science*, Vol. 25, N 3-4, 2001, pp. 183-192.
- [21] S. Jugjai, A. Sawananon, The surface combustor-heater with cyclic flow reversal combustion embedded with water tube bank, *Fuel*, Vol. 83, 2004, pp. 2369-2379.
- [22] Jun-Rui Shi, Mao-Zhao Xie, Gang Li, Hong Liu, Ji-Tang Liu, Hong-Tao Li, Approximate solutions of lean premixed combustion in porous media with reciprocating flow, *International Journal of Heat and Mass Transfer*, vol. 52, 2009, pp. 702-708.
- [23] Liming Du, Maozhao Xie, The Influences of Thermophysical Properties of porous Media on superadiabatic Combustion with Reciprocating Flow, *Heat Transfer-Asian Research*, Vol. 35, N 5, 2006, pp. 336-350.
- [24] Katsunori Hanamura, Tomoyuki Kumano, Yuya Iida, Electric power generation by super-adiabatic combustion in thermoelectric porous element, *Energy*, Vol. 30, 2005, pp. 347-357.
- [25] Loy Chuan Chia, Bo Feng, The development